Dominant failure mode analysis using representative samples obtained by multiple response surfaces method

Youbao Jiang[a*]; Linjie Zhao[a]; Michael Beer[b,c]; Lei Wang[a]; Jianren Zhang[a]

(a School of Civil Engineering, Changsha University of Science and Technology, Changsha 410114, China;

b Institute for Risk and Reliability, Leibniz Universität Hannover, Hannover, Germany;

c Institute for Risk & Uncertainty, University of Liverpool, Liverpool L69 3GQ, UK)

Abstract: The conventional methods for failure mode analysis usually fail to identify dominant failure modes efficiently for large structures. To overcome this issue, an approach based on representative samples is proposed, which combines the MRS (multiple response surfaces) method with iterative strategies. The main steps are: (1) use MRS method to approximate the system failure function piecewise and to search the multiple design points; (2) perform deterministic structural analysis to identify failure sequences for samples in the important domain rather than the total domain; (3) solve representative samples with iterative strategies to obtain a converged solution based on a visualization plot. A key merit of this approach is that it can identify dominant failure modes efficiently due to the utilization of samples with most contributions to system failure, such as design points, etc. Numerical examples show that the proposed method can be used well to search dominant failure modes for structures.

Key words: structural reliability; multiple response surfaces; failure mode; representative samples; reliability plot; sector division

*Corresponding author

E-mail address: youbaojiang@hotmail.com

1 Introduction

For complex engineering structures or systems with uncertainties, the identification of dominant failure modes can provide valuable information for achieving a safe design and for accurate reliability estimation. In recent years, significant attention has been paid to the dominant failure mode analysis and reliability estimation of structures and systems with uncertainties [1-3]. Two representative methods: analytical methods [4-15] and simulation methods [16-27]) have been developed greatly to meet the target.

The analytical methods usually use deterministic mechanical analyses and failure probability computations to search failure modes, including criterion methods [4,5], branch and bound methods [6-11], incremental loading methods [12-14] and approaches based on mathematical programming [15], et al. For example, the optimality criterion method (reported by Feng [5]) uses the means of variables (i.e. a deterministic way) to identify the critical failure modes among the innumerable possible failure modes. Moreover, the branch and bound method usually uses failure probability analyses continuously to search each failure member until system failure. This often needs time-consuming computations of failure probability of dominant failure modes in the event tree due to statistical dependency of the obtained failure modes. For example, Lee and Song [7] developed an improved branch and bound method (termed the B^3 method), which can search the dominant failure modes efficiently and can estimate the system-level risk accurately. Generally, the analytical methods can deal with system reliability problems elegantly, but one of the main shortcomings is that it needs a great number of failure sequences to be considered especially for a large structural system with many structural elements and a long failure path.

The simulation methods including Monte Carlo simulation (MCS) [21-23], adaptive importance sampling schemes [24], and genetic algorithms (GA) [25-27], et al. can provide a statistical estimation of dominant failure modes by sampling. However, there are still some problems when applied to a large structural system with high level reliability. For example, a great number of simulations have to be performed for the crude Monte Carlo simulation; a "good" sampling density function is usually difficult to select due to multiple failure sequences involved for the adaptive importance sampling schemes. These problems mainly result from the fact that most of the randomly generated samples are in the safe region, which do not lead to a system failure and also do not contribute to the failure mode identification. For this sake, Neves et al. [21] reported an improved method, which uses limit state sample points to construct a local response surface for each failure mode and to identify the dominant failure modes.

However, for these simulation-based approaches above, the sample points are usually randomly generated rather than elaborately designed. This leads to low efficiency in searching the representative sample points corresponding to dominant failure modes, which only occupy a small proportion of all sample points. Actually, if the unnecessary computations (e.g. nonlinear mechanical analyses for sample points corresponding to negligible failure modes) are reduced to the maximum extent, the computational efficiency can be improved largely for dominant failure mode analysis. Since the nonlinear mechanical analysis is the most time-consuming task among all computations, in particular when large structural systems are considered, the associated cost can be saved dramatically by reducing the number of nonlinear analyses.

Herein, we proposed an improved method for searching the dominant failure modes with small number of nonlinear structural analyses. It mainly uses targeted deterministic mechanical analyses

for representative sample points to satisfy this demand. The proposed approach combines the multiple response surfaces (MRS) method with an iterative algorithm to obtain the representative sample points. Finally, its efficiency and accuracy are discussed through examples in Section 4.

2 Samples and failure modes

2.1 Limit state sample points

Following the common simulation-based approaches, the sample points are usually generated randomly. Therefore, most of the sample points are in the safe region with significant likelihood, and no system failure can be identified after a nonlinear mechanical analysis in this case, which leads to unnecessary computations.

Herein, a simple technique is introduced for limit state sample points. To illustrate this idea, consider a simple case with two basic variables: resistance R and load S. Let $P_0(R_0, S_0)$ be a common sample point, then the limit state sample points is acquired with the fixed resistance R_0 and limit load $S_{\lim}$ (solved by structural analysis or finite element simulations), which is denoted by $P(R_0, S_{\lim})$, as shown in Fig.1.

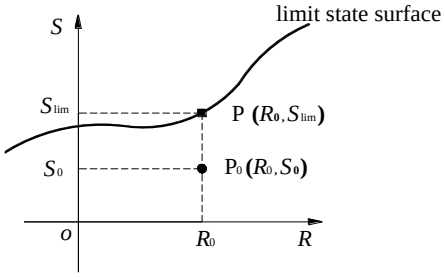

Fig.1 Limit state sample points for two basic variables

Generally, there are many variables for structures and systems. Let y_1, y_2,$\cdots$, y_{n_1} and y_{n_1+1}, y_{n_1+2},$\cdots$, $y_{n_1+n_2}$ be n_1 resistance variables and n_2 load variables, respectively, then the resistance vector $\boldsymbol{R}$ and load vector $\boldsymbol{S}$ are given by

$$\boldsymbol{R} = [y_1, y_2, \cdots, y_{n_1}] \tag{1}$$

$$\boldsymbol{S}=[y_{n_1+1}, y_{n_1+2}, \cdots, y_{n_1+n_2}] \tag{2}$$

Without loss of generality, choose y_{n_1+1} as the scaling factor, and the load ratio vector $\boldsymbol{r}_{\mathrm{L}}$ is given by

$$\boldsymbol{r}_{\mathrm{L}}=[1, y_{n_1+2}/y_{n_1+1}, \cdots, y_{n_1+n_2}/y_{n_1+1}] \tag{3}$$

Then, for a structure with given $\boldsymbol{R}$ and $\boldsymbol{r}_{\mathrm{L}}$, a limit load factor F_{lim} can be identified through a nonlinear mechanical analysis. Thus, the limit state sample point can be specified by

$$\mathrm{SP}=\left\{y_1, y_2, \cdots, y_{n_1}, F_{\mathrm{lim}}[1, \frac{y_{n_1+2}}{y_{n_1+1}}, \cdots, \frac{y_{n_1+n_2}}{y_{n_1+1}}]\right\} \tag{4}$$

2.2 Failure modes identification based on samples

Once a limit state sample point is selected, then all the structural variables have corresponding deterministic values. Thus, a deterministic mechanical analysis can be performed and the failure sequence can be identified easily.

For example, consider a one-story and one-bay frame as shown in Fig.2. It has four elements: E1-E4 with sectional properties given in Tab.1. Assume that the stress-strain relationship is ideal elastic-plastic for the frame material, and the yield strength is 276MPa, and the elastic modulus is 210GPa. The applied concentrated forces (F_1 and F_2) and the moment capacities (M_1 for E1 and E4, and M_2 for E2 and E3) are assumed to be statistically independent. Their statistics are shown in Tab.2, in which the COV denotes coefficient of variation.

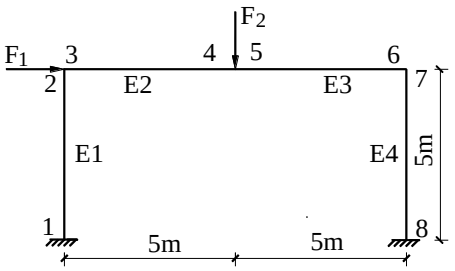

Fig.2 One-story and one-bay frame

Tab.1 Sectional properties of elements

Elements	A/m^2	I/m^4
E1, E4	4×10^{-3}	3.58×10^{-5}
E2, E3	4×10^{-3}	4.77×10^{-5}

Note: A is cross section area; I is moment of inertia, the same below.

Tab.2 Statistics of variables for frame

Variables	Distribution	Mean	COV
M_1	Normal	75kN•m	5×10^{-2}
M_2	Normal	101kN•m	5×10^{-2}
F_1	Normal	20kN	0.3
F_2	Normal	40kN	0.3

If five representative samples are selected as listed in Tab.3, then based on these samples, the corresponding failure sequences can be identified with mechanical analyses, as shown in Fig.3.

Tab.3 Representative samples and failure modes

Sample No.	M_1/kN•m	M_2/kN•m	F_1/kN	F_2/kN	Failure mode
1	74.44	99.84	21.20	70.24	Fig.3(a)
2	74.44	108.52	24.86	70.12	Fig.3(b)
3	72.04	104.38	15.86	77.80	Fig.3(c)
4	80.96	92.47	10.94	78.64	Fig.3(d)
5	70.95	106.96	3.32	80.20	Fig.3(e)

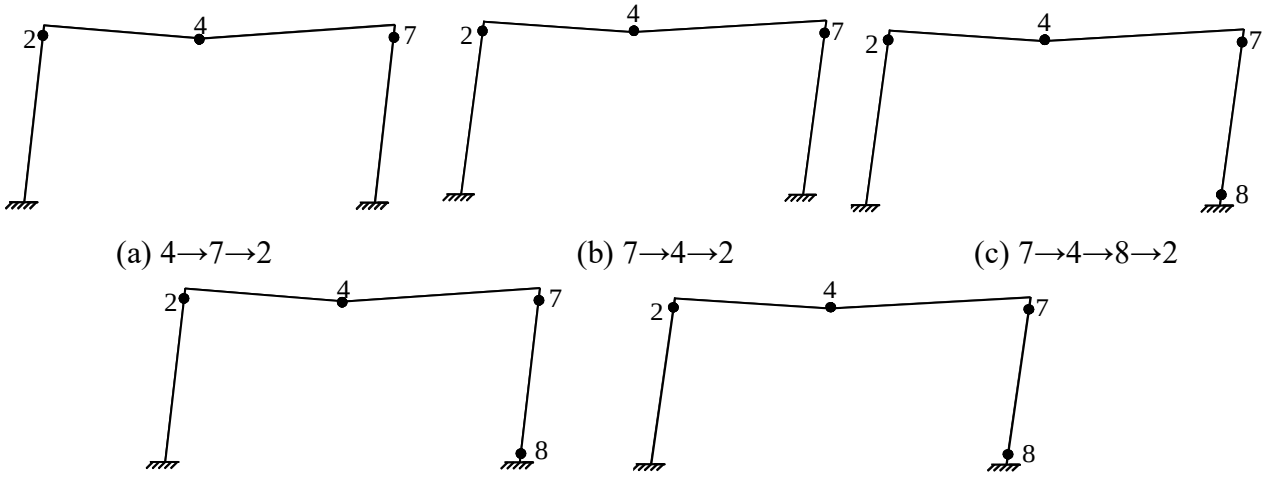

(a) 4→7→2 (b) 7→4→2 (c) 7→4→8→2

(d) 4→7→8→2 (e) 7→8→4→2

Fig.3 Failure modes based on the representative samples

In fact, many researchers have carried out a failure mode analysis for this classical example. For example, Kim et al. [28] used a total of 2,270,000 Monte Carlo simulations to obtain a system reliability index 2.4697 and the first five failure modes: 4→7→2, 7→4→2, 7→4→8→2, 4→7→8→2, and 7→8→4→2. By comparison, the five dominant failure modes obtained with the 5 representative samples are the same as those obtained with the huge number of Monte Carlo simulations reported by Kim et al. [28].

It is noteworthy that the representative samples are actually selected from a certain number of sample points. So, to improve searching efficiency, the proportion of representative samples with respect to the total samples needs to be increased dramatically. Herein, the response surface method and iterative schemes are used to obtain these representative samples efficiently.

3 Dominant failure mode analysis

3.1 Multiple response surfaces method

As well known, the limit state function is usually implicit for practical structures. In this case, response surface methods [29-36] have been widely applied for reliability analysis, which can provide an approximate explicit function model. Most of them are applied to problems involving single or multiple limit states, but seldom applied to problems involving multiple failure sequences (mixed failure mechanisms). Jiang et al. [29] proposed a multiple response surfaces (MRS) method to deal with this issue. Examples show that the MRS method can be applied well for complex (high dimensional, piecewise and nonlinear) limit-state surfaces in design points searching and reliability calculation. Herein, a brief introduction of the MRS method is described.

Let $\Phi(\cdot)$ denote the cumulative distribution function (CDF) of standard normal variable, and

n denote the variable number, $n=n_1+n_2$. For a variable y_j with CDF $F_{cd}(\cdot)$, the corresponding standard normal variable x_j can be given by

$$x_j = \Phi^{-1}[F_{cd}(y_j)] \quad j = 1, 2, \cdots, n \tag{5}$$

The inverse transformation is given as

$$y_j = F_{cd}^{-1}[\Phi(x_j)] \quad j = 1, 2, \cdots, n \tag{6}$$

With Eq.(5), all variables can be transformed into standard normal ones. In standard normal space, let $\boldsymbol{x}_0$ be the closest sample point (i.e. converged design point finally) to the origin, which also regarded as a vector $\boldsymbol{x}_0$. Then, an inner product coefficient can be defined as

$$\rho_0(\boldsymbol{x}) = (\boldsymbol{x}_0 \cdot \boldsymbol{x}) / \|\boldsymbol{x}_0\| / \|\boldsymbol{x}\| \tag{7}$$

Numerical examples in [29] shows that this coefficient can be used efficiently to divide the space into sectors, especially for high-dimensional (e.g. as many as 20 variables) cases. For example, s sectors are obtained based on the selected coefficients ρ_i, as shown in Fig.4, in which the i^{th} sector is defined as:

$$\rho_i \le \rho_0(\boldsymbol{x}) \le \rho_{i-1} \quad i = 1, 2, \cdots, s \tag{8}$$

where ρ_0=1.0 for the first sector.

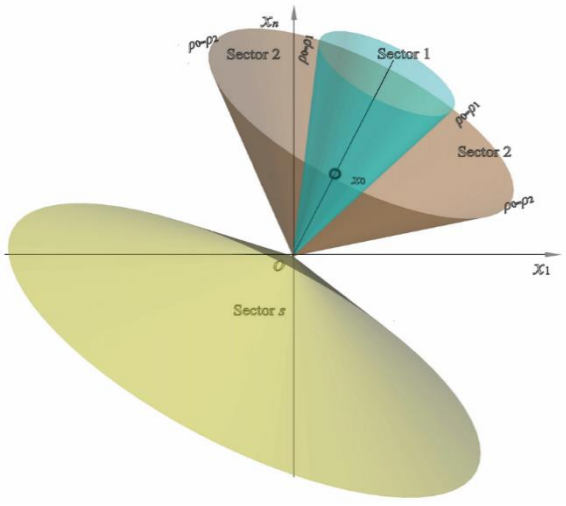

Fig.4 Diagram of sector division technique

In each sector, a response surface is used for function fitting and the number of sample points are selected elaborately for zero residual fitting purpose. For example, if the quadratic polynomials are selected for response surface fitting, then the limit state equation for each sector can be given by

$$Z = 1 + \sum_{j=1}^{n} a_j x_j + \sum_{j=1}^{n} b_j x_j^2 = 0 \tag{9}$$

where a_j and b_j are coefficients. Herein, $2n$ sample points are selected in each sector to achieve the targeted zero residual fitting, for there are $2n$ coefficients in Eq.(9) (without cross terms) needed to be determined.

For MRS method, if s sectors are selected, then s corresponding response surfaces are used for function fitting. With increasing sector number actively, it can achieve the zero residual fitting easily for cases with large number of samples, and thus can approximate the real function accurately.

3.2 Generation of critical samples

The sample points closer to the origin usually correspond to the dominant failure modes. Thus, efficient generation of such critical sample points is the key to search the dominant failure modes. This is similar to search design points by iterative sampling with a response surface method, where more and more sample points close to the origin are obtained in iterative searching until the converged design points are sufficiently accurate. For a complex engineering structure or system failure, it usually involves a solution of multiple design points [37-38], which would require an accurate and efficient response surface method to execute reliability analysis.

The critical samples including multiple design points can be obtained with the following steps: (1)Select a suitable uniform table $U_c(q^g)$ (c, q, and g are table parameters, see [33]) to generate initial samples in $\boldsymbol{x}$ space by Eq.(10), with which the initial data can be distributed uniformly in design space.

$$x_{ij} = \lambda[2(u_{ij} - 1)/(q - 1) - 1] \tag{10}$$

where u_{ij} is a value within [1, q] in the uniform table; and λ is a range parameter with λ=2.0 to 3.0 for usual cases [33,39].

(2)Transform the initial samples into $\boldsymbol{y}$ space with Eq.(6), and then use Eq.(4) in Section 2.1 to acquire limit state sample points.

(3)Obtain the $\boldsymbol{x}$ space sample points with the $\boldsymbol{y}$ space sample points and Eq.(5) transformation, and use MSR method to perform a function fitting, and search the multiple design points.

(4)Transform the currently searched multiple design points into $\boldsymbol{y}$ space with Eq.(6), and check whether they are on the limit state surface by structural analyses. If yes, go to step (6); if not, go to step (5).

(5)Generate sample points with the searched design points by using Eq.(4) in Section 2.1. Add the generated sample points to update the current sample point sets, and go to step (3).

(6)Record all the obtained sample points (including the converged design points) as a basic set for failure mode and reliability analysis later.

With the converged design points, the system failure function is expressed explicitly in piecewise form with response surfaces in all sectors. Since the evaluation of the response surfaces is very fast, even the crude MCS can be selected to calculate the failure probability, circumventing the construction of importance sampling density functions etc. Furthermore, the crude MCS with large number of samples is usually considered as an accurate method for complex limit state functions. Herein, the crude MCS is adopted and the corresponding flowchart is given in Fig. 5. This procedure delivers the system failure probability P_{f} as well as the failure modes. Then, the system reliability can be calculated as

193 $$\beta = -\Phi^{-1}(P_f) \tag{11}$$

194 where β is the system reliability index. Note that P_f and β are required for the following failure

195 mode searching. For example, as shown in Eq.(14), P_f is used to define the important domain, in

196 which the representative samples corresponding to the dominant failure modes are searched.

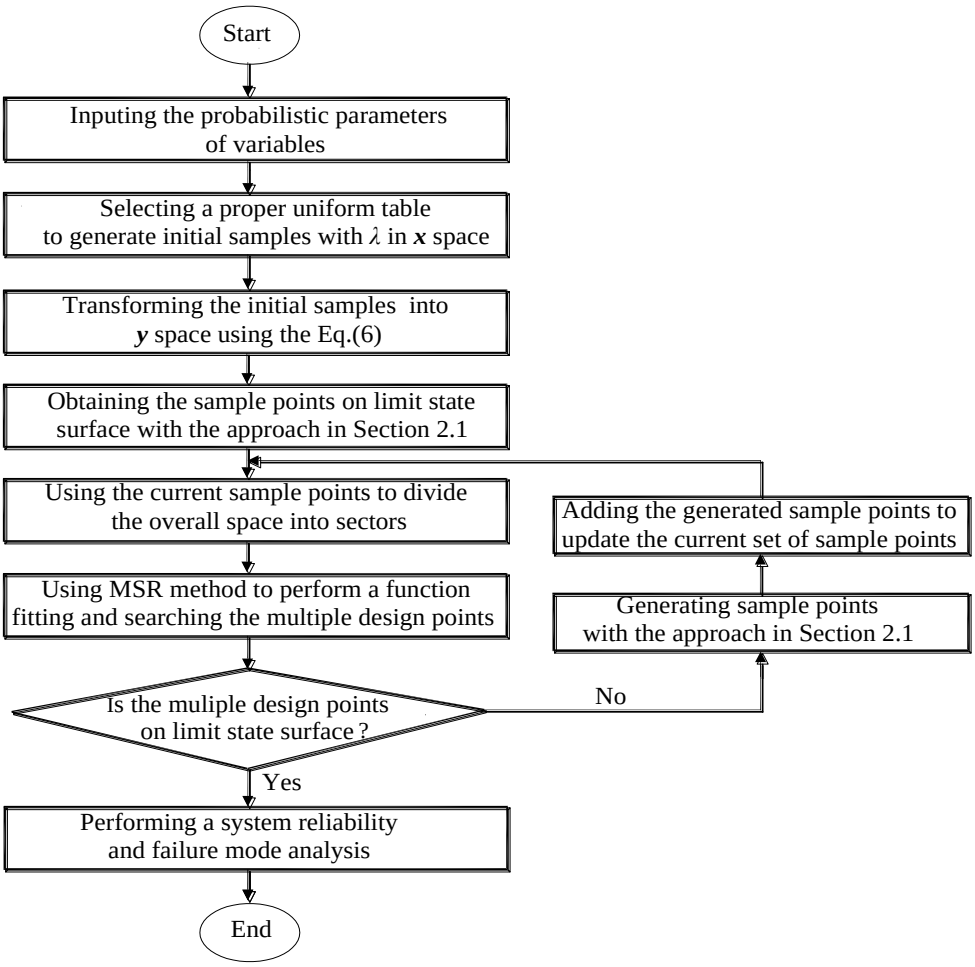

197

198 Fig.5. Solution flowchart of critical samples including design points with MRS method

199 ***3.3 Strategies for searching dominant failure mode***

200 When a limit state sample point is obtained through a deterministic structural analysis, the failure

201 mode can also be identified. Hence, both failure mode and its location in space are known for a given

202 sample point.

203 Due to the large number of failure modes for complex engineering systems, some critical sample

points, which correspond to dominant failure modes, would not be included in basic sample set (i.e. samples obtained in Section 3.2). Herein, a practical iterative strategy is proposed to search more dominant failure modes possibly. This strategy is based on a visualization plot approach for reliability problems proposed by Hurtado [40]. The approach introduces two parameters d and r for a reliability plot, which are defined as:

$$d = \sqrt{\sum_{j=1}^{n} x_j^2} \tag{12}$$

$$r = (\boldsymbol{x}^* \cdot \boldsymbol{x}) \Big/ \left\| \boldsymbol{x}^* \right\| \Big/ \left\| \boldsymbol{x} \right\| \tag{13}$$

where $\boldsymbol{x}^*$ is the closest design point.

With this approach, the samples can be labeled with different types of failure mode in a d-r 2D visualization. For each type of sample points, its representative sample point is defined as the one with the least d value. For reliability problems, a sphere domain with a smaller d value ($d<d_{\mathrm{cr}}$), namely important domain, often contributes most significantly to the total failure probability, and d_{cr} is estimated by:

$$\mathrm{P}(d^2 > d_{\mathrm{cr}}^2) = \varepsilon P_{\mathrm{f}} \tag{14}$$

where ε is a parameter, ε=0.01～0.1 for most cases. This indicates that the probability of the samples (both failure and safe samples) outside the important sphere domain is only $\varepsilon P_{\mathrm{f}}$, and the probability of the failure samples outside the important sphere domain should be less than $\varepsilon P_{\mathrm{f}}$. Thus the failure modes corresponding to these failure samples also contribute less to the total failure probability, and they can be neglected for dominant failure mode searching.

Based on representative sample points, such important domain can be divided into multiple sub-domains (SD) by selected ranges of r. Then, check the distributions of sample points in each sub-

domain. If a much larger difference of r for two adjacent sample points appears in one sub-domain, then some additional sample points (ASPs) are added in this sub-domain to search possible dominant failure modes, as shown in Fig.6.

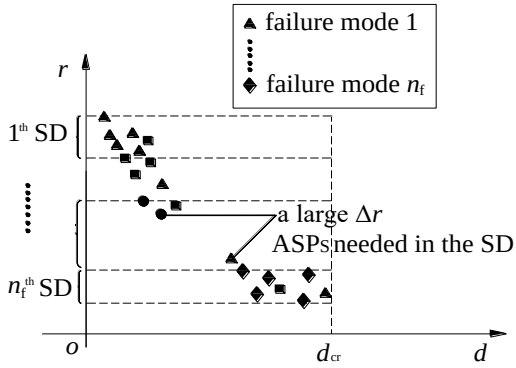

Fig.6. Sub-domain divisions in important domain

The main steps for searching dominant failure modes are as follows:

(1)Identify failure modes for the basic set of sample points obtained in Section 3.2. Set i=0.

(2)Record the number of different failure modes as $n_f^{(i)}$, and find out the representative sample point with the least d value for each type of failure mode. Thus, $n_f^{(i)}$ representative sample points are obtained.

(3)Select $n_f^{(i)}$ ranges of r based on $n_f^{(i)}$ representative sample points, and divide the important domain into $n_f^{(i)}$ sub-domains.

(4)Let Δr be the maximum difference of r between two adjacent samples for each sub-domain. Check whether $\Delta r^{(l)}$ is much larger for the l^{th} sub-domain, l=1, 2,⋯, $n_f^{(i)}$. If not, go to step (7); if yes, go to step (5).

(5)Use the Eq.(15) to generate some tentative sample points (TSP) linearly between two representative sample points.

$$\boldsymbol{x}_{\text{TSP},k} = \boldsymbol{x}_l + \frac{k}{h+1}(\boldsymbol{x}_{l+1} - \boldsymbol{x}_l)(k \in [1,h]) \tag{15}$$

where $\boldsymbol{x}_l$ is the l^{th} representative sample point; $\boldsymbol{x}_{l+1}$ is the $(l+1)^{\text{th}}$ representative sample point ($l<n_f^{(i)}$) or the sample point with the least r in sub-domain ($l=n_f^{(i)}$); h is the number of TSP needed in iterative steps, and usually h=4~8.

For each TSP, use the approach proposed in Section 2.1 to obtain an ASP on the limit state surface and its corresponding failure mode through a deterministic structural analysis.

(6)Update the current sample set with the location and failure mode type of the obtained ASPs, $i=i+1$; go to step (2).

(7)Identify the dominant failure modes with the representative sample points obtained finally.

Generally, the failure modes are much less than sample points, since many sample points usually correspond to the same failure mode. To obtain a more accurate reliability result, all the sample points can be used to update the system failure function fitting with MRS method after the dominant failure mode converged. Finally, the system reliability can be updated, too.

Note that the proposed failure mode searching approach uses the MRS method to obtain representative sample points and adopts iterative calculations rather than less efficient sampling schemes (e.g. MCS) to identify failure modes. As a main advantage of this approach, the failure mode can be searched much more efficiently. This is demonstrated in the following examples.

4 Examples

4.1 Frame structure (*Example 1*)

Consider a one-story two-bay frame subjected to concentrated horizontal and vertical forces (F_1 and F_2) in Fig.7. Assume that stress-strain relationship is ideal elastic-plastic for the frame material with the yield strength 296MPa and the elastic modulus 210GPa. The frame members use common

sections from the AISC [41], as shown in Tab.4. The forces and the moment capacities (M_1 for beams and M_2 for columns) are statistically independent. Their statistics are given in Tab.5. Assume that only bending failure is defined for failure mode analysis.

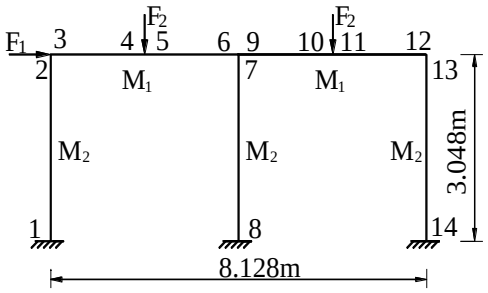

Fig.7. A one-story two-bay frame

Tab.4 Sectional parameters of the frame structure

Members	Section	A/m^2	I/m^4
beams	W16×57	1.084×10^{-2}	3.16×10^{-4}
columns	W14×53	1.006×10^{-2}	2.25×10^{-4}

Tab.5 Statistics of variables for the frame structure

Variable	Distribution	Mean	COV
M_1	Normal	448.44kN•m	0.15
M_2	Normal	371.99kN•m	0.15
F_1	Normal	266.89kN	0.3
F_2	Normal	444.82kN	0.3

The limit state function can be considered as:

$$Z=\left\{[F_{\lim}(M_1,M_2)-F_2]\middle|\boldsymbol{r}_{\mathrm{L}}=[1,F_1/F_2]\right\}=0 \tag{16}$$

For this example with 4 normal variables, a uniform table of $U^*_{48}(48^4)$ is selected to generate initial samples with λ=3.0. The corresponding values of $\boldsymbol{y}=[y_1, y_2, y_3, y_4]=[M_1, M_2, F_1, F_2]$ are obtained based on Eq.(6). Using ANSYS software, $F_{\lim}$ is solved by deterministic failure analysis for each sample. Then, 48 limit state sample points are obtained correspondingly with Eq.(4) and they are transformed into $\boldsymbol{x}$ space (standard normal) with Eq.(5).

Using the obtained 48 initial limit state samples, the overall standard normal space is divided

into 6 sectors. Then, a response surface function is obtained and the design point is searched in each sector. It is found that the currently obtained design points do not satisfy the requirements for convergence. Thus, these design points are used to generate 6 samples. These 6 generated sample points are added to update the sample points for iterative calculations. After 1 iterative step, it is found that the 6 newly generated design points satisfy the requirements for convergence. The coefficients of the 6 response surfaces in $\boldsymbol{x}$ space are shown in Tab.6. Thus, there are 60 sample points in total (including the converged 6 design points) in the basic sample set.

The system failure function can be expressed explicitly in a piecewise form with response surfaces in 6 sectors. The system failure probability is 1.7×10^{-3} calculated by MCS.

Tab.6 Coefficient of multiple response surfaces function for Example 1

MRS No.	x_1	x_1^2	x_2	x_2^2	x_3	x_3^2	x_4	x_4^2
1	0.064	-0.013	-0.011	-0.005	-0.017	-0.049	-0.018	-0.101
2	-0.031	-0.044	-0.062	-0.158	0.017	-0.100	-0.044	-0.223
3	-0.042	-0.060	0.016	-0.014	-0.025	-0.023	-0.019	-0.097
4	-0.029	-0.067	-0.007	0.015	-0.039	-0.024	-0.018	-0.104
5	0.068	-0.032	0.034	-0.030	-0.023	-0.030	-0.034	-0.094
6	-0.041	-0.088	0.036	0.067	0.003	-0.047	-0.313	-0.031

In the standard normal space, the obtained 60 basic sample points are sorted from small to large according to their d value. Then, the critical distance for the important domain is determined as $d_{cr}=5.08$ with $\varepsilon=0.02$. It is found that there are only 36 sample points in the important domain among the 60 basic sample points. The 36 sample points are sorted from large to small according to the r value, and their corresponding failure modes are also identified through deterministic structural analyses.

In the d-r 2D visualization plot, the 36 sample points are labeled with different failure modes. 4 sample points are selected as representative sample points as shown in Tab.7. Based on these 4

representative sample points, the important domain can be divided into 4 sub-domains by 4 selected ranges of r ([1.0, 0.94], [0.94, 0.85], [0.85, 0.60], [0.60, 0.37]) with Δr =0.01, 0.03, 0.09, 0.11, respectively.

It is observed that the Δr in both the third sub-domain and the fourth sub-domain is much larger than that in other sub-domains. We use Eq.(15) to add 4 tentative sample points in both the third sub-domain and the fourth sub-domain. For each tentative sample point, we use the proposed approach in Section 2.1 to obtain an ASP on the limit state surface and to identify its corresponding failure mode through a deterministic structural analysis. Updating the current sample set with the location and failure mode type of the obtained 8 ASPs, it is observed that no new failure mode is searched, and the dominant failure mode searching converges with 44 samples in total in the important domain, and Δr =0.01, 0.03, 0.04, 0.04 in 4 sub-domains, respectively, as shown in Fig.8. Therefore, the 4 most dominant failure modes are identified based on the plastic mechanism analysis, as illustrated in Fig.9.

Tab.7 Representative samples corresponding to the dominant failure modes

Sample No.	M_1/kN•m	M_2/kN•m	F_1/kN	F_2/kN	Failure mode
1	416.82	356.92	274.90	842.49	Fig.9(a)
12	515.03	324.00	266.09	845.16	Fig.9(b)
18	467.95	412.72	357.37	842.49	Fig.9(c)
27	420.86	452.34	470.26	783.77	Fig.9(d)

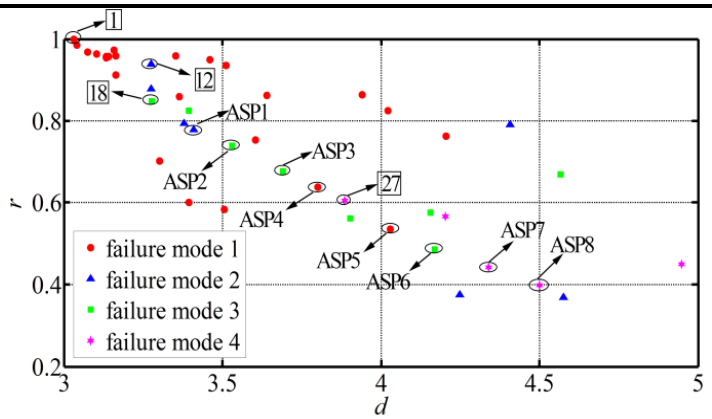

Fig.8. 4 representative samples with numbers boxed among 44 samples in important domain

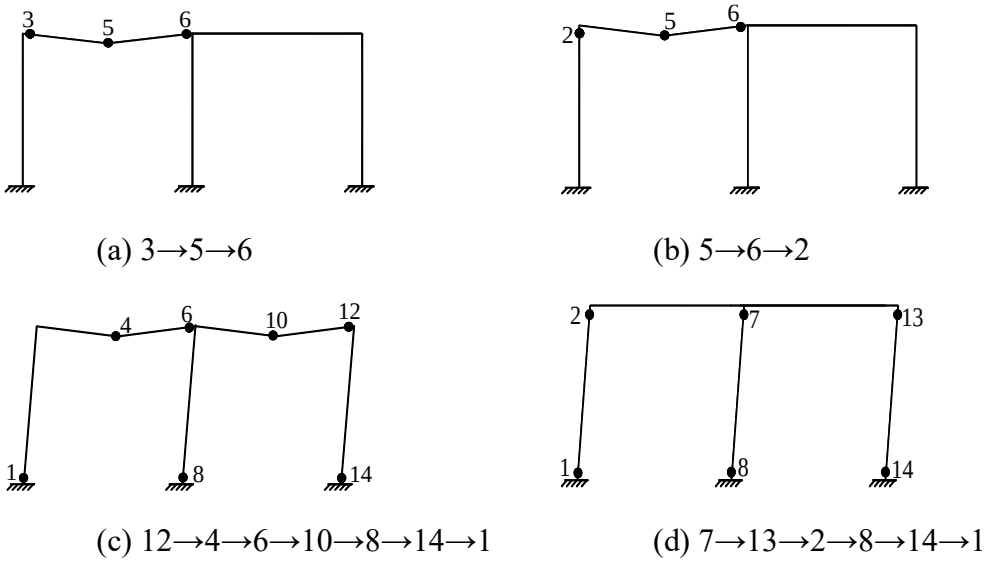

(a) 3→5→6 (b) 5→6→2

(c) 12→4→6→10→8→14→1 (d) 7→13→2→8→14→1

Fig.9. Dominant failure modes based on the representative samples.

This example was also analyzed previously by other researchers. Dey et al. [24] used a total of 210 simulations of structural analyses to obtain the reliability and failure modes results. The 4 dominant failure modes in Fig.9 are the same as those reported by Dey et al. [24]. However, the proposed method only needs 68 finite element analysis (FEA) calls (60 calls for basic sample set, and 8 calls for 8 ASPs) to search dominant failure modes.

Furthermore, the direct MCS is also used to obtain analysis results with a total of 3.0×10^4 simulations. The reliability results are summarized in Tab.8. Compared with the other two methods, the proposed method shows clear advantages in numerical efficiency.

Tab.8 Comparisons between reliability results for the frame

Method	No. of structural simulations	P_f	β
Proposed method	68	1.7×10^{-3}	2.93
MCS	3.0×10^4	2.3×10^{-3}	2.83
Method [24]	210	2.1×10^{-3}	2.86

4.2 Six-bar truss structure (*Example 2*)

Consider a six-bar truss subjected to five forces (F_1, F_2,⋯, F_5) with height 0.9m and width 1.2m

reported by Kim et al. [28], as shown in Fig.10. The stress-strain relationship is assumed as ideal elastic-plastic for the truss material. All the members have the same section area A=2.3×10^{-4} m^2 but different yield strengths, σ_{yi} (i=1,⋯,6). Suppose that the concentrated forces and yield strengths are all independent random variables. The statistics of variables are summarized in Tab.9.

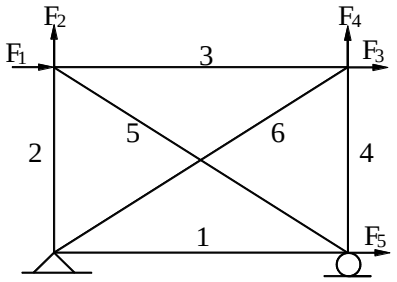

Fig.10. Statically indeterminate six-bar truss.

Tab.9 Statistics of variables for the truss

Variables	Distribution	Mean	COV
F_1	Normal	50kN	0.1
F_2	Normal	30kN	0.1
F_3	Normal	20kN	0.1
F_4	Normal	30kN	0.1
F_5	Lognormal	20kN	0.1
σ_{yi} (i=1,⋯,6)	Normal	276MPa	0.05

For this case, there are 11 variables. Herein, a uniform table of $U^*_{88}(88^{11})$ is selected to generate initial samples, where λ=2.0 for variable σ_{yi} (i=1,⋯,6) and λ=3.0 for variable F_i (i=1,⋯,5), respectively. The corresponding values of $\boldsymbol{y}$=[y_1, y_2,⋯, y_{10}, y_{11}]=[F_1, F_2,⋯, σ_{y5}, σ_{y6}] are obtained based on Eq.(6). Then, the limit load is solved with ANSYS for each sample. The 88 limit state sample points are obtained with Eq.(4) and transformed into $\boldsymbol{x}$ space (standard normal) with Eq.(5).

With these 88 initial samples, 4 sectors are obtained by dividing the overall standard normal space. In each sector, the corresponding function fitting is performed and the design point is searched. It is found that the solutions have converged after 7 iterative steps, and there are 120 sample points

343 (including the converged four design points) in total in the basic sample set.

344 The system failure function can be expressed explicitly in a piecewise form with response
345 surfaces in 4 sectors. The system failure probability is 1.2×10^{-3} calculated by MCS.

346 In $\boldsymbol{x}$ space, the obtained 120 basic sample points are sorted from small to large according to their
347 d value. Then, the critical distance for the important domain is determined as d_{cr}=6.42 with ε=0.02. It
348 is found that there are only 56 sample points in the important domain among the 120 basic sample
349 points. The 56 sample points are sorted from large to small according to the r value, and their
350 corresponding failure modes are identified through deterministic structural analysis.

351 In the d-r 2D visualization plot, the 56 sample points are labeled with different failure modes. 3
352 sample points are selected as the representative sample points as shown in Tab.10. Based on the 3
353 representative sample points, the important domain can be divided into 3 sub-domains by 3 selected
354 ranges of r ([1, 0.8], [0.8, 0.57], [0.57, 0.29]) with Δr =0.07, 0.05, 0.07, respectively.

355 It is observed that the Δr values in the 3 sub-domains are smaller and close to each other, and
356 the dominant failure mode searching converges obviously (no iterations needed), as shown in Fig.11.
357 The three most dominant failure modes of the truss are: (6→2), (6→1), (2→6) based on the plastic
358 mechanism analysis.

359 Kim et al [28] used 2840 simulations of structural analyses to identify 3 dominant failure modes.
360 However, this method only needs 120 FEA calls to identify 3 dominant failure modes, which are the
361 same as those reported in [28]. Thus, the proposed method improves the efficiency dramatically. For
362 the purpose of comparison, MCS is performed and the failure probability is 1.3×10^{-3} obtained by
363 2.5×10^{4} simulations. Then, the reliability results are shown in Tab.11.

364 Tab.10 Representative samples corresponding to the dominant failure modes

Sample No.	Load/kN					Yield strength/MPa						Failure mode
	F_1	F_2	F_3	F_4	F_5	σ_{y1}	σ_{y2}	σ_{y3}	σ_{y4}	σ_{y5}	σ_{y6}	
1	59.0	34.0	22.0	30.9	20.3	276.4	274.8	268.0	261.4	272.3	255.9	6→2
11	63.8	32.9	22.1	30.3	23.3	262.6	276.3	278.8	259.7	276.3	262.6	6→1
36	66.2	34.8	24.4	30.2	21.7	273.1	282.2	309.3	276.8	274.9	275.0	2→6

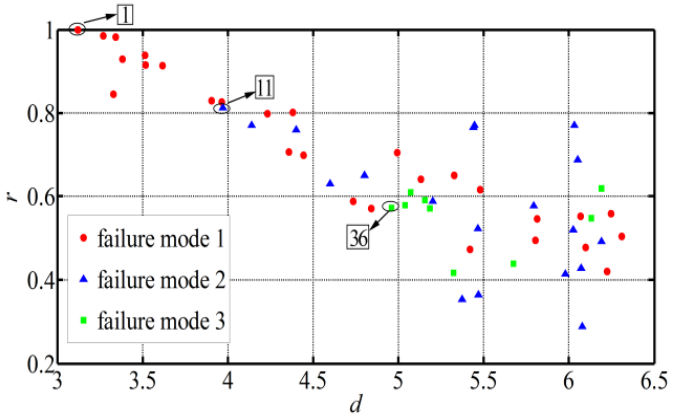

Fig.11. 3 representative samples with numbers boxed among 56 samples in important domain

Tab.11 Comparisons between reliability results for the truss

Method	No. of structural simulations	P_f	β
Proposed method	120	1.2×10^{-3}	3.04
Reference [28]	2840	1.4×10^{-3}	2.98
MCS	2.5×10^{4}	1.3×10^{-3}	3.01

4.3 Truss bridge structure (*Example 3*)

Consider a 2-D truss bridge with 25 members. It is subjected to two forces P_1 and P_2 as shown in Fig.12. The section areas are given in Tab.12. The stress-strain relationship is assumed as ideal elastic-plastic for the truss material with yield strengths of the members, σ_{yi} (i=1,⋯,25). Suppose that the concentrated forces and yield strengths are all independent variables. Tab.13 summarizes the statistics of variables.

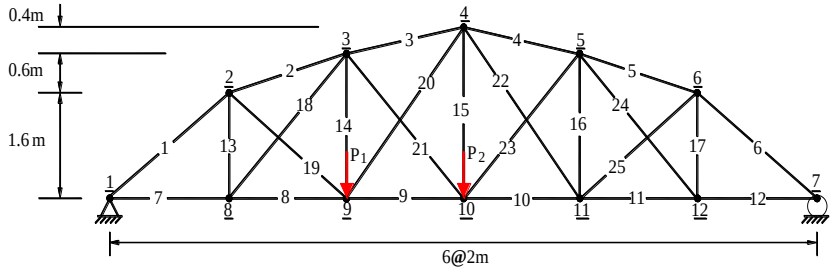

Fig. 12. A truss bridge structure.

Tab.12 Section areas of 25 members for the truss bridge

No. of members	A/m^2
1-6	15×10^{-4}
7-12	14×10^{-4}
13-17	12×10^{-4}
18-25	13×10^{-4}

Tab.13 Statistics of variables for the truss bridge

Variable	Distribution	Mean	COV
P_1	Lognormal	160kN	0.1
P_2	Lognormal	160kN	0.1
σ_{yi} (i=1,⋯,25)	Normal	276MPa	0.05

For this case, there are 27 variables. A uniform table of $U^*_{162}(162^{27})$ is selected. Using Eq.(10), the generate initial samples are obtained with λ=2.0 and λ=3.0 for x_{ij} variables corresponding to yield strength variables and load variables, respectively. Then, the corresponding values of $\boldsymbol{y}$=[y_1, y_2,⋯, y_{26}, y_{27}]=[σ_{y1}, σ_{y2},⋯, P_1, P_2] are obtained based on Eq.(6). The limit load is solved by a deterministic analysis with ANSYS for each sample. The 162 limit state sample points are acquired with Eq.(4) and they are transformed into $\boldsymbol{x}$ space (standard normal) with Eq.(5).

Using these 162 initial samples, 3 sectors are obtained by dividing the overall standard normal space. Then, the design point is searched for each response surface function obtained by zero residual fitting. The solutions have converged after 2 iterative steps. This leads to 171 sample points in total (including the converged three design points) in the basic sample set.

388 The system failure function can be expressed explicitly in a piecewise form with response
389 surfaces in 3 sectors. The system failure probability is 6×10^{-3} calculated by MCS.

390 In $\boldsymbol{x}$ space, the obtained 171 basic sample points are sorted from small to large according to their
391 d value. Then, the critical distance for the important domain is determined as d_{cr}=7.91 with ε=0.02. It
392 is found that there are 140 sample points in the important domain among the 171 basic sample points.
393 The 140 sample points are sorted from large to small according to the r value, and their corresponding
394 failure modes are identified through deterministic structural analysis.

395 In the d-r 2D visualization plot, the 140 sample points are labeled with different failure modes.
396 8 sample points are identified as the representative ones. With these 8 representative sample points,
397 the important domain can be divided into 8 sub-domains by selected ranges of r ([1,0.69], [0.69,0.50],
398 [0.50,0.49], [0.49,0.48], [0.48,0.45], [0.45,0.44], [0.44,0.35], [0.35, 0.28]) with Δr =0.21, 0.13, 0.01,
399 0.01, 0.003, 0.002, 0.01, 0.02, respectively.

400 It is observed that the Δr in the first sub-domain and the second sub-domain is much larger than
401 that in other sub-domains. We use Eq.(15) to add 8 tentative sample points in the first sub-domain
402 and 4 tentative sample points in the second sub-domain. For each tentative sample point, we use the
403 proposed approach from Section 2.1 to obtain an ASP on the limit state surface and to identify its
404 corresponding failure mode through a deterministic structural analysis. Updating the current sample
405 set with the location and failure mode type of the newly obtained 12 ASPs, it is observed that no new
406 failure mode is searched, and the dominant failure mode searching converges with 152 samples in
407 total in the important domain, and Δr =0.03, 0.04, 0.01, 0.01, 0.003, 0.002, 0.01, 0.02 in 8 sub-
408 domains respectively, as shown in Fig.13. Tab.14 summarizes the representative sample points
409 labeled with failure modes.

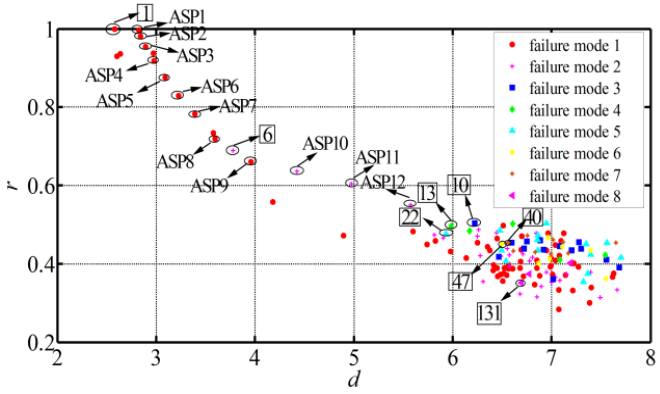

Fig.13. 8 representative samples with numbers boxed among 152 samples in important domain

Kim et al [28] also analyzed this example and identified 10 dominant failure modes through 51, 344 simulations of structural analyses. Herein, 8 dominant failure modes are identified using only 183 FEA calls (171 calls for basic sample set, and 12 calls for 12 ASPs) with this method, which are among the 10 failure modes reported in [28]. The failure mode analysis results are shown in Tab.15.

Tab.15 Comparisons of failure modes for the truss bridge

Reference [28]	Proposed method	
failure modes	failure modes	Sample No.
3→9	3→9	1
9→3	9→3	6
3→2→9	2→3→9	10
2→3→9	9→2→3	13
2→9→3	3→2→9	22
9→2→3	3→1	40
1	3→4→9	47
3→4→9	4→3→9	131
3→1		
4→3→9		

The 2 failure modes (2→9→3, 1) that are found by Kim et al [28] but not by our approach contribute less to the total failure probability. Thus, it leads to a smaller difference between P_f results (see P_f results in Tab.16). That is, our approach concentrates on the most significant failure modes resulting a great gain in efficiency, but sacrificing accuracy only marginally. The efficiency of

searching dominant failure modes is improved dramatically by solving the representative sample points. Furthermore, the direct MCS is also performed and P_f is 6.7×10^{-3} obtained by a total of 2.0×10^{4} simulations. The reliability results are shown in Tab.16.

Tab.16 Reliability results for the truss bridge

Method	No. of structural simulations	P_f	β
Proposed method	183	6×10^{-3}	2.51
Reference [28]	51,344	5.4×10^{-3}	2.55
MCS	2.0×10^{4}	6.7×10^{-3}	2.47

4.4 25-bar truss structure (*Example 4*)

To check its applicability for a structural system with some more complex functionality and smaller failure probabilities, a 25 bar space truss (high voltage transmission tower, see [42]) with the horizontal load F_1 and the vertical load F_2 is considered, as shown in Fig.14. The section areas of 25 members are given in Tab.17. The stress-strain relationship is assumed as ideal elastic-plastic for the truss material with elastic modulus 2.06×10^{5} MPa. The loads and the yield stresses of the members, σ_{yi} (i=1,⋯,25), are considered as random variables. Suppose that they are all independent and their statistics are listed in Tab.18.

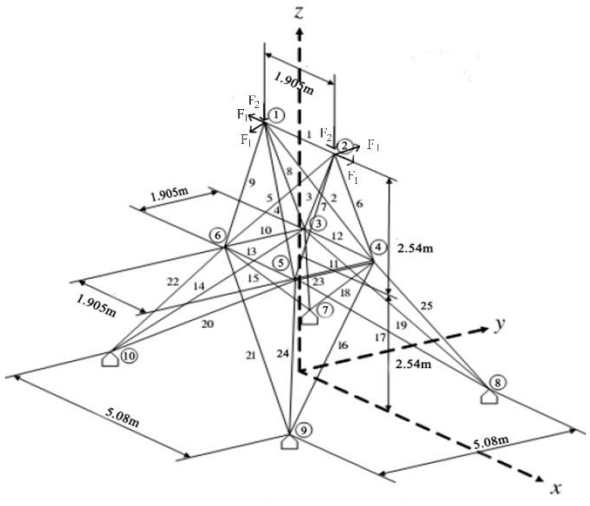

Fig. 14. Space truss with 25 members.

Tab.17 Cross section areas of members

Type	Ⅰ	Ⅱ	Ⅲ	Ⅳ	Ⅴ	Ⅵ	Ⅶ	Ⅷ	Ⅸ	Ⅹ	Ⅺ	Ⅻ	ⅩⅢ
No. of Members	1	2	3	6	7	10	12	14	15	18	19	22	23
		5	4	9	8	11	13	17	16	21	20	25	24
A/cm^2	4.36	4.56	7.47	2.39	7.52	1.51	1.77	4.88	1.89	1.78	2.63	4.89	7.66

Tab.18 Statistics of random variables

Variable	Distribution	Mean	COV
F_1	Normal	88.9kN	0.2
F_2	Normal	22.6kN	0.2
σ_{yi} (i=1,⋯,25)	Normal	276MPa	0.05

Firstly, 162 initial samples are selected by uniform design, and the limit load is solved through elasto-plastic analysis for each sample. Using the obtained 162 initial samples, 3 sectors are obtained by dividing the overall standard normal space. Following the procedure as shown in Example 3, the solutions have converged after 1 iterative step. There are 168 sample points in total (including the converged three design points) in the basic sample set.

The system failure function can be expressed explicitly in a piecewise manner with response surfaces in 3 sectors. The system failure probability is 1.43×10^{-6} computed by MCS.

In $\boldsymbol{x}$ space, the obtained 168 basic sample points are sorted from small to large with respect to their d value. Then, the critical value for the important domain is determined as d_{cr}=9.40 with ε=0.02. It is found that there are only 78 sample points in the important domain among the 168 basic sample points. The 78 sample points are sorted from large to small according to the r value, and their corresponding failure modes are identified through deterministic structural analysis.

In the d-r 2D visualization plot, the 78 sample points are labeled with different failure modes. 9 sample points are selected as the representative sample points. Based on these representative sample

points, the important domain can be divided into 9 sub-domains by selected ranges of r ([1,0.98], [0.98,0.64], [0.64,0.61], [0.61,0.60], [0.60,0.58], [0.58,0.576], [0.576,0.54], [0.54,0.535], [0.535,0.42]) with Δr =0.02, 0.29, 0.02, 0.01, 0.01, 0.003, 0.01, 0.002, 0.06, respectively.

It is observed that the r differences in both the second sub-domain (Δr=0.29) and the ninth sub-domain (Δr=0.06) are much larger. Using Eq.(15) we add 8 tentative sample points in the second sub-domain and 4 tentative sample points in the ninth sub-domain. For each tentative sample point, we use the proposed approach from Section 2.1 to obtain an ASP on the limit state surface and to identify its corresponding failure mode by a deterministic structural analysis. Updating the current sample set with the location and failure mode types of the newly obtained 12 ASPs, it is observed that no new failure mode is searched, and the dominant failure mode searching converges with 90 samples in the important domain in total, and Δr =0.02, 0.04, 0.02, 0.01, 0.01, 0.003, 0.01, 0.002, 0.03 in 9 sub-domains, respectively, as shown in Fig.15.

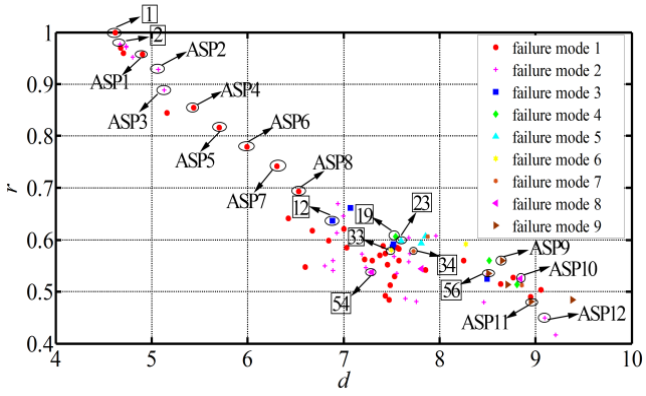

Fig.15 9 representative samples with numbers boxed among 90 samples in important domain

Dong [42] used the branch and bound method to obtain 24 failure modes for this example and computes the failure probability as [0.99×10^{-6}, 1.0×10^{-6}] with the narrow reliability bounds method proposed by Ditlevesen [43]. However, the proposed method required a total of 180 calls (168 calls for basic sample set, and 12 calls for 12 ASPs) of structural analysis to obtain P_f as 1.43×10^{-6} and to

identify nine dominant failure modes, which are the same as the first 9 failure modes reported in [42]. The failure modes analysis results are shown in Tab.19.

Tab.19 Comparisons of failure modes for the truss tower

	Proposed method	Branch and bound method [42]
Sample No.	Dominant failure modes	Dominant failure modes
1	3→6	3→6
2	4→9	4→9
12	7→9→17	7→9→17
19	3→10→12	3→10→12
23	4→11→13	4→11→13
33	3→11→9	3→11→9
34	4→10→6	4→10→6
54	3→10→1	3→10→1
56	4→10→13	4→10→13

Then, the comparisons between reliability results are shown in Tab.20. The obtained result of system failure probability matches well with the MCS result. The proposed method identifies, again, the most important failure modes with a big gain in efficiency sacrificing accuracy only marginally.

Tab.20 Reliability results for the truss tower

Method	No. of structural simulations	P_f
Proposed method	180	1.43×10^{-6}
MCS	2×10^{7}	1.17×10^{-6}
Reference [42]	–	$[0.99\times10^{-6}, 1.0\times10^{-6}]$

4.5 Summary

Conventional methods (e.g. analytical methods and simulation-based methods) are usually less efficient in searching dominant failure modes for large structures. However, the proposed method can efficiently achieve the goals by solving multiple design points with the MRS method and by obtaining the representative samples in the important domain with iterative strategies. Moreover, if with a large

number of samples, the searched dominant failure modes can be usually accurate.

With numerical examples, it is known that the proposed method are applied well to identifying dominant failure modes, especially suitable for large structures, because it needs much less computational effort to obtain similar accurate reliability results in most cases.

5 Conclusions

An approach based on representative samples is proposed to identify failure modes. It combines the MRS method, iterative strategies and visualization plot techniques to improve the efficiency of searching dominant failure modes. The conclusions are drawn as follows:

(1) Combining the MRS method with other techniques (e.g. limit state sample points), the system failure function can be expressed explicitly in a piecewise manner, and the basic sample set including the converged multiple design points can be obtained efficiently.

(2) Considering contributions of samples to failure probability, the sample points in the important domain rather than in the total domain are used for identifying failure sequences, and they can be labeled with different failure modes in a 2D visualization plot.

(3) With the distribution of sample points in important domain, iterative strategies (e.g. sub-domain division, adding additional sample points) are adopted to search a converged solution of the representative samples corresponding to the dominant failure modes. The result converges quickly and stably verified by examples.

(4) Based on the representative samples, the method can be applied well to identifying dominant failure modes in most cases, even with a smaller number of structural simulations, and thus especially suitable for large structures.

Acknowledgement

The research is supported by the National Natural Science Foundation of China (Grant No.51678072, 51778068), and Key Discipline Foundation of Civil Engineering of Changsha University of Science and Technology (18ZDXK01).

References:

[1] Freudenthal AM, Garrelts JM, Shinozuka M. The analysis of structural safety. Journal of Structures Division, ASCE 1966; 92: 267–325.

[2] Thoft-Christensen P, Baker MJ. Structural reliability theory and its applications. Springer-Verlag; 1982.

[3] Melchers RE. Structural reliability: analysis and prediction. 2nd ed New York, NY: John Wiley; 1999.

[4] Song B F, Feng Y S. The influence of failure mode order on structural system reliability. Computers & Structures, 1990, 34(1): 17-22.

[5] Feng Yuansheng. Enumerating significant failure modes of a structural system by using criterion methods. Computers and Structures, 1988, 30(5): 1152-1157.

[6] Srividya A, Ranganathan R. Automatic generation of stochastically dominant failure modes in frame structures for reliability studies. Reliability Engineering & System Safety, 1992, 37(1): 15-23.

[7] Lee YJ, Song J. Risk analysis of fatigue-induced sequential failures by branch-and-bound method employing system reliability bounds (B3 method). ASCE Journal of Engineering Mechanics 2011; 137(12): 807–21.

524 [8] Lee YJ, Song J. Finite-element-based system reliability analysis of fatigue- induced sequential
525 failures. Reliability Engineering & System Safety 2012; 108: 131–41.
526 [9] Murotsu Y, Okada H, Taguchi K, Grimmelt M, Yonezawa M. Automatic generation of
527 stochastically dominant failure modes of frame structures. Structural Safety 1984; 2: 17–25.
528 [10] Thoft-Christensen P, Murotsu Y. Application of structural systems reliability theory. Berlin:
529 Springer-Verlag; 1986.
530 [11] Karamchandani A. Structural system reliability analysis methods. Report no. 83. Department of
531 Civil Engineering, Stanford University; 1987.
532 [12] Lee JS. Basic study on the reliability analysis of structural systems. Journal of Ocean Engineering
533 and Technology 1989; 12: 145–57.
534 [13] Moses F, Stahl B. Reliability analysis format for offshore structures. In: Proceedings of the 10th
535 annual offshore technology conference, 1978; Paper 3046.
536 [14] Moses F. System reliability developments in structural engineering. Structural Safety 1982; 1:
537 3–13.
538 [15] Corotis RB, Nafday AM. Structural system reliability using linear programming and simulation.
539 Journal of Structural Engineering ASCE 1989; 115(10): 2435-47.
540 [16] Ditlevsen O, Bjerager P. Plastic reliability analysis by directional simulation. Journal of
541 Engineering Mechanics ASCE 1989; 115(6): 1347–62.
542 [17] Grimmelt M, Schueller GI. Benchmark study on methods to determine collapse failure
543 probabilities of redundant structures. Structural Safety 1982; 1: 93–106.
544 [18] Rashedi MR. Studies on reliability of structural systems. Department of Civil Engineering, Case
545 Western Reserve University; 1983.

546 [19] Moses F, Fu G. Important sampling in structural system reliability. Fifth ASCE EMD/GTD/STD
547 specialty conference on probabilistic mchanics; 1988.
548 [20] Melchers RE. Structural system reliability assessment using directional simulation. Structural
549 Safety 1994; 16: 23–37.
550 [21] Neves Rodrigo A, Mohamed-Chateauneuf Alaa, Venturini Wilson S. Component and system
551 reliability analysis of nonlinear reinforced concrete grids with multiple failure modes. Structural
552 Safety, 2008, 30(3): 183-199.
553 [22] Naess A, Leira B J, Batsevych O. Reliability analysis of large structural systems. Probabilistic
554 Engineering Mechanics, 2012, 28: 164–168
555 [23] Song J, Ok SY. Multi-scale system reliability analysis of lifeline networks under earthquake
556 hazards. Earthquake Engineering and Structural Dynamics 2010, 39(3): 259–79.
557 [24] Dey A, Mahadevan S. Ductile structural system reliability analysis using adaptive importance
558 sampling. Structural Safety 1998; 20(2): 137–154.
559 [25] Shao S, Murotsu Y. Approach to failure mode analysis of large structures. Probabilistic
560 Engineering Mechanics 1999; 14: 169–77.
561 [26] Holland JH. Adaptation in natural and artificial systems. Ann Arbor: University of Michigan
562 Press; 1975.
563 [27] Goldberg GE. Genetic algorithms in search, optimization and machine learning. Reading, MA:
564 Addison-Wesley; 1989.
565 [28] Kim D S, Ok S Y, Song J, et al. System reliability analysis using dominant failure modes
566 identified by selective searching technique. Reliability Engineering and System Safety, 2013, 119:
567 316–331.

568 [29] Jiang Y, Zhao L, Beer M, et al. Multiple response surfaces method with advanced classification
569 of samples for structural failure function fitting. Structural Safety, 2017, 64:87-97.
570 [30] Roussouly N, Petitjean F, Salaun M. A new adaptive response surface method for reliability
571 analysis. Probabilistic Engineering Mechanics 2013, 32(2): 103-115.
572 [31] Zhao W, Qiu Z. An efficient response surface method and its application to structural reliability
573 and reliability-based optimization. Finite Elements in Analysis and Design, 2013, 67: 34-42.
574 [32] Bucher C G, Most T. A comparison of approximate response functions in structural reliability
575 analysis. Probabilistic Engineering Mechanics 2008, 23(2): 154-163.
576 [33] Jiang Y, Luo J, Liao G, et al. An efficient method for generation of uniform support vector and
577 its application in structural failure function fitting. Structural Safety, 2015, 54: 1-9.
578 [34] Donald E. Brown, Jeffrey B. Schamburg. A generalized multiple response surface methodology
579 for complex computer simulation applications. Proceeding of the 2004 Winter Simulation
580 Conference[C], 2004: 958-966.
581 [35] Li DQ, Jiang SH, Cao ZJ, et al. A multiple response-surface method for slope reliability analysis
582 considering spatial variability of soil properties. Engineering Geology, 2015, 187: 60–72.
583 [36] Li L, Chu X. Multiple response surfaces for slope reliability analysis. International Journal for
584 Numerical and Analytical Methods in Geomechanics, 2015, 39(2): 175–192.
585 [37] Der Kiureghian A, Dakessian T. Multiple design points in first and second-order reliability.
586 Structural Safety, 1998, 20(1): 37-49.
587 [38] Haukaas T, Der Kiureghian A. Strategies for finding the design point in non-linear finite element
588 reliability analysis. Structural Safety, 2006, 21(2): 133-147.
589 [39] Cheng J, Li Q S, Xiao R. A new artificial neural network-based response surface method for

590 structural reliability analysis. Probabilistic Engineering Mechanics, 2008, 23(1): 51-63.
591 [40] Hurtado Jorge E. Dimensionality reduction and visualization of structural reliability problems
592 using polar features. Probabilistic Engineering Mechanics 2012, 29: 16–31.
593 [41] Manual of steel construction: load and resistance factor design. Chicago. (IL): American Institute
594 of steel construction, 1986.
595 [42] Dong C. System reliability theories and their applications to modern structures. Beijing: Science
596 Press, 2001. (in Chinese).
597 [43] Ditlevsen O. Narrow reliability bounds for structural system. Journal of Structural Mechanics,
598 1979, 7(4): 453-472.

599 Tab.14 Representative samples corresponding to the dominant failure modes

Variable	Sample No.							
	1	6	10	13	22	40	47	131
σ_{y1}/MPa	275.72	272.96	301.53	302.63	285.11	263.17	254.61	284.69
σ_{y2}/MPa	274.62	273.79	300.84	295.32	299.18	257.65	270.62	248.40
σ_{y3}/MPa	267.72	270.48	277.93	261.10	272.69	255.30	274.48	271.03
σ_{y4}/MPa	272.41	277.66	269.65	265.51	249.37	293.94	296.01	283.04
σ_{y5}/MPa	273.38	275.31	280.00	263.86	288.56	269.65	270.62	299.87
σ_{y6}/MPa	274.90	277.24	266.62	297.80	262.75	270.62	288.83	268.27
σ_{y7}/MPa	278.21	281.11	281.38	287.87	252.13	265.93	276.14	281.93
σ_{y8}/MPa	276.83	275.86	254.20	271.03	259.03	286.76	265.24	252.54
σ_{y9}/MPa	275.03	273.93	252.13	250.06	283.73	288.83	297.11	280.00
σ_{y10}/MPa	275.45	276.97	280.97	280.00	257.65	280.69	262.75	279.31
σ_{y11}/MPa	276.97	275.72	295.04	268.27	266.89	272.69	283.04	266.62
σ_{y12}/MPa	274.21	279.45	289.94	283.31	271.72	252.13	275.17	281.93
σ_{y13}/MPa	274.21	275.03	266.20	252.13	266.62	270.62	254.20	259.03
σ_{y14}/MPa	264.55	230.87	289.52	257.37	271.31	302.63	288.83	297.39
σ_{y15}/MPa	276.41	276.00	287.18	290.90	254.89	280.69	257.37	284.42
σ_{y16}/MPa	272.96	278.76	259.72	265.93	274.48	262.48	258.34	276.14
σ_{y17}/MPa	277.10	277.52	281.66	271.31	261.10	258.06	250.06	284.42
σ_{y18}/MPa	275.59	275.59	277.93	271.03	256.96	265.93	300.84	291.59
σ_{y19}/MPa	278.90	283.59	273.79	287.87	284.00	296.70	291.32	257.37
σ_{y20}/MPa	276.97	276.28	276.14	299.18	270.34	270.07	255.58	251.44
σ_{y21}/MPa	277.66	278.07	277.93	290.21	273.79	248.68	284.42	279.31
σ_{y22}/MPa	274.90	279.04	256.96	299.87	273.10	262.75	276.83	274.48
σ_{y23}/MPa	276.83	275.17	295.32	268.69	256.68	264.13	269.65	272.69
σ_{y24}/MPa	274.62	278.21	273.10	268.00	265.93	250.75	278.62	262.06
σ_{y25}/MPa	276.14	279.17	288.83	276.83	273.10	272.41	295.73	252.54
P_1/kN	118.41	112.01	126.77	123.93	141.00	141.53	133.88	163.75
P_2/kN	29.79	26.94	36.52	27.48	28.39	31.19	34.04	24.50
Failure mode	3→9	9→3	2→3→9	9→2→3	3→2→9	3→1	3→4→9	4→3→9

600